1 Introduction

The goal of this project is to construct the propagation of quantum optical modes through a linear optical circuit (referred to as LOC from now on), constructed from beam splitters and phase shifters. We then project the final state onto a desired Fock outcome to find the probability. For Fock state inputs, such a process is related to *boson sampling* - a classically hard problem first proposed by Aaronson and Arkhipov[1]. For Gaussian-state inputs involving squeezing and displacement, the problem is related to *Gaussian boson sampling* proposed by Hamilton *et al.*[2].

While the original boson sampling problem was designed to show quantum advantage with no actual applications in mind, Gaussian boson sampling, is closely related to computationally difficult problems such as graph-related algorithms and quantum chemistry (see [3] for an in-depth review of such applications). Hence, the classical simulation of such propagation holds value in finding quantum-inspired algorithms for tackling these problems.

We develop a universal method to calculate the propagation through a linear optical circuit using *tensor networks*, which can effectively represent a many-body system satisfying the area-law of entanglement. We specifically focus on the ability to effectively compress many-body quantum states using MPS (matrix product states) and matrix-vector multiplication using efficient MPO (matrix product operators) - MPS contraction.

2 Methods

2.1 Backward Propagation in Heisenberg Picture

This section provides a method to propagate a single input Fock state through an arbitrary linear optical circuit. Such a process is useful as we are interested in problems where we project the final state onto a Fock state.

$$|\langle \mathbf{n}_{\text{fin}}|\mathcal{U}|\psi_{\text{init}}\rangle|^2 \tag{1}$$

where $|\psi_{\text{init}}\rangle$ is any state that can effectively be represented as an MPS, $|\mathbf{n}_{\text{fin}}\rangle = |n_1, \ldots, n_L\rangle$ is a Fock state, and $\mathcal{U}$ is an L-mode unitary operator in many-body basis that represents linear optical circuit. If we can propagate a single Fock state, then we can efficiently calculate Eq.(1) by 'reverse propagating' the final state, i.e.,

$$|\langle \mathbf{n}_{\text{fin}}|\mathcal{U}|\psi_{\text{init}}\rangle|^2 = \left|\langle \mathcal{U}^\dagger \mathbf{n}_{\text{fin}}|\psi_{\text{init}}\rangle\right|^2$$

A propagation through a linear optical circuit in terms of the creation and annihilation operators can be considered as a change of basis.

$$b_\mu = U_{\mu\nu} a_\nu$$

Now consider an output Fock state $|\mathbf{n}\rangle = |n_1, \ldots, n_L\rangle$. In the original basis we know that the Fock state is constructed in the form

$$|\mathbf{n}\rangle = \prod_\mu \frac{1}{\sqrt{n_\mu!}} (a_\mu^\dagger)^{n_\mu} |0\rangle$$

After transforming the basis, the state becomes

$$\mathcal{U}^\dagger |\mathbf{n}\rangle = \prod_\mu \frac{1}{\sqrt{n_\mu!}} (b_\mu^\dagger)^{n_\mu} |0\rangle = \prod_\mu \frac{1}{\sqrt{n_\mu!}} (U_{\mu\nu}^* a_\nu)^{n_\mu} |0\rangle \tag{2}$$

To perform this calculation, we follow the 'Fermi sea' creation process in Wu *et al.*[4]. We first construct an MPO for each creation operator $b_\mu^\dagger$, then sequentially apply the MPO to a vacuum state MPS. Since each creation operator is defined as a linear combination of local operators, they can be converted to an MPO with bond dimension $D = 2$ as

$$b_\mu^\dagger = \begin{pmatrix} U_{\mu\nu}^* a_\nu^\dagger & I \end{pmatrix} \left[\prod_\nu \begin{pmatrix} I & O \\ U_{\mu\nu}^* a_\nu^\dagger & I \end{pmatrix} \right] \begin{pmatrix} I \\ U_{\mu\nu}^* a_\nu^\dagger \end{pmatrix}$$

It is then straightforward to construct the state Eq.(2) by applying each creation MPO sequentially to a vacuum state. For instance, for the initial state $|\mathbf{n}\rangle = |n_1, \ldots, n_L\rangle$, then we apply the $b_1^\dagger$ MPO n_1 times, $b_2^\dagger$ MPO n_2 times, ... See (a) of fig.1 for a tensor network diagram of the process.

Because the bond dimension increases exponentially, we must truncate the contracted MPS. A simple method to perform this task is to use truncated SVD for all sites. However, since the MPO $b_\mu^\dagger$ updates **all** sites, naive truncation leads to great errors, hence leading to a need for a greater bond dimension to reduce errors. The SVD method's accuracy is determined by the entanglement entropy of MPS. Plotting the entanglement entropy reveals that SVD truncation leads to large errors. Indeed, we observe in 5 that the relative error of this method requires a large maximum bond dimension to provide accurate results (see (b) of 1 for the direct plotting of the entanglement entropy increase for each step).

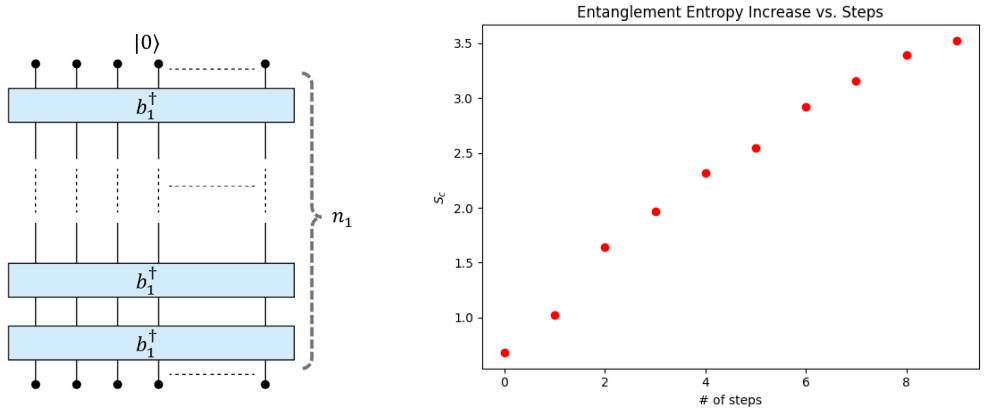

(a) TN diagram for MPO applications

(b) S_c increase vs. Steps

Figure 1: (a) Tensor network diagram for sequential MPO applications (b) Entanglement entropy at the middle site for sequential MPO applications.

Therefore, we implement a DMRG-styled sweeping variational algorithm that effectively approximates the MPO-MPS contraction. We mainly follow the algorithm proposed in

Ayral *et al.*[5], which was adjusted to adapt to the bosonic basis of our problem. We apply such DMRG algorithms after applying each $(b_\mu^\dagger)^{n_\mu}$. Before stating the full algorithm, we state the notations used. First, each $b_\mu^\dagger$ MPO is denoted as B_μ, with the τ-th site tensor being $B_\mu^{(\tau)}$. We denote the MPO-MPS contraction as a simple matrix-matrix multiplication. We denote the MPS form of the contracted tensor up to the p-th creation operator as M_p, i.e.,

$$M_p = \prod_{\mu=1}^{p} \frac{1}{\sqrt{n_\mu!}} (B_\mu)^{n_\mu} |0\rangle$$

The tensor for the τ-th site of M_p is $M_p^{(\tau)}$.

Now, we state the DMRG algorithm. First contract the creation MPO B_μ, n_μ times with the MPS $M_{\mu-1}$, resulting in an MPS with large bond dimension, denoted as $B_\mu^{n_\mu} M_{\mu-1}$. We want to find a suitable approximation for this MPS with a lower bond dimension, i.e.,

$$M_\mu \sim B_\mu^{n_\mu} M_{\mu-1}$$

For each sweep, we optimize one site $M_\mu^{(\tau)}$ while keeping the other tensors fixed. We contract $B_\mu^{n_\mu} M_{\mu-1}$ and M_μ **excluding** $M_\mu^{(\tau)}$ and denote the contracted tensor as $F_\mu^{(\tau)}$. Now we maximize the overlap $\mathrm{Tr}\, F_\mu^{(\tau)} M_\mu^{(\tau)*}$ while maintaining normalization conditions. The optimal tensor $M_\mu^{(\tau)}$ becomes

$$\max M_\mu^{(\tau)} = \frac{F_\mu^{(\tau)}}{\sqrt{\mathrm{Tr}\, F_\mu^{(\tau)} F_\mu^{(\tau)*}}}$$

(see [5] for further details). During the sweeping process, we store left and right contracted results for improved performance. The total pseudocode for the DMRG styled bond dimension the reduction is stated below, where some of the notations are rephrased for clearer code.

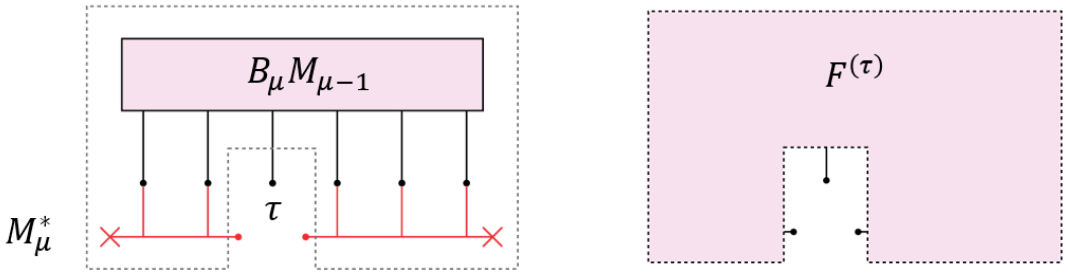

(a) $B_\mu M_{\mu-1}$, M_μ^* without $M_\mu^{(\tau)*}$ (b) Contracted $F_\mu^{(\tau)}$

Figure 2: (a) The tensor network diagram for $F_\mu^{(\tau)}$ (b) The contracted result for $F_\mu^{(\tau)}$

We estimated the time complexity of the proposed process. First we look at the MPO-MPS contraction. There are L sites and for each site, we contract a degree-3 tensor with

Algorithm 1 Variational DMRG algorithm for bond dimension reduction

$M \leftarrow B$ ▷ Initialize M by setting it to the contracted MPS
$F_r[end] \leftarrow 1$ ▷ Initialize F_r by setting it to all right contracted tensors
for $i =$ end to 1 **do**
  $F_r[i] \leftarrow \text{updateRight}(F_r[i+1], M[i+1], B[i+1])$
end for
$F_l \leftarrow 1$ ▷ We iteratively update F_l by updating from the left side
for $i = 1$ to end **do**
  if $i > 1$ **then**
    $F_l \leftarrow \text{updateLeft}(F_l, M[i-1], B[i-1])$
  end if
  $F \leftarrow \text{contract}(F_l, B[i], F_r)$
  $M[i] \leftarrow F/\sqrt{\text{Tr}\, FF^*}$ ▷ Normalization
  $M[i], S, V \leftarrow \text{svd}(M[i])$
  if $i < L$ **then**
    $M[i+1] \leftarrow \text{contract}(SV, M[i+1])$
  else
    $M[i] \leftarrow \text{contract}(M[i], V)$ ▷ At the end, there is only one singular value
  end if
end for

size $[D, D, N+1]$ (assuming the worst case, being that the MPS bond dimensions are fully saturated) and a degree-4 tensor with size $[N+1, N+1, 2, 2]$ (each creation MPO is a locally acting MPO; hence the bond dimension is 2). The initial MPO-MPS contraction requires $O(D^2N^2)$, and contracting the two right and left legs with the identity to create single leg each require $O(D^3N)$ floating-point operations. Since we perform this process for n_μ times, the total time complexity is approximately $O(2^{3n_\mu}D^3NL)+O(2^{3n_\mu}D^2N^2L)$. Thus, the approximate number of floating point operations are polynomial with respect to D and N, and proportional to $\sum_\mu \exp n_\mu$. This hints at an exponential increase in performance where the desired Fock outputs are distributed evenly compared to sharp distributions, but we have not found a way to properly benchmark the output distribution relation with time.

2.2 Forward Propagation Through LOC Elements

We now propose another method, which more closely resembles the propagation through linear optical components (beam splitters and phase shifters). We first note that an arbitrary unitary $L \times L$ unitary matrix can be decomposed into $L(L-1)/2$ $SU(2)$ unitaries, that act on adjacent modes. The specific procedures to perform this decomposition was first given by Reck[6] then subsequently improved upon (in terms of fidelity and robustness) by Clements[7]. Such a process is covered in appendix A and implemented using the Python package, *Strawberry Fields*[8].

Similar to the method before, we limit the bosonic Fock space to the total number of photons in the desired output. Each linear optical element is constructed into a locally acting MPO

in Fock space. In the Clements design, each $SU(2)$ element consists of one beam splitter and two phase shifters, resulting in two degrees-of-freedom.

Each $SU(2)$ element in Fock space can be considered as a unitary propagator of an arbitrary two-site, tight-binding Hamiltonian.

$$\mathcal{U}_{\mathrm{BS}}(\theta,\phi) = \exp\left(e^{i\phi}\theta a_1^\dagger a_2 - e^{-i\phi}\theta a_2^\dagger a_1\right) \tag{3}$$

For a limited number of photons, such an expression can be explicitly calculated in the Fock basis. Using the rectangular decomposition function of Strawberry Fields, we can obtain the various phase values θ_j and ϕ_j for the j-th $SU(2)$ element (where $j = 1, 2, \ldots, L(L-1)/2$). We use these values to calculate the matrix representation of $\mathcal{U}_{\mathrm{BS}}$ in Fock basis, then apply it to the adjacent sites. We apply the traditional SVD method to locally truncate the bond dimensions of the affected sites.

3 Results

We first benchmarked the error rate with respect to the maximum bond dimension. First, to calculate the hafnian efficiently, we utilize the Python package *thewalrus*[9]. We fix the inputs and desired outputs, and then calculate the probability of measuring such an output. We use single-mode squeezed input states without displacement to reduce the computational cost of benchmarking.

$$S[\mathbf{r}]\,|0\rangle = \bigotimes_{j=1}^{L}\left[\frac{1}{\sqrt{\cosh r_j}}\sum_{n=0}^{\infty}(-e^{i\phi}\tanh r_j)^n\frac{\sqrt{(2n)!}}{2^n n!}\,|2n\rangle\right]$$

Due to limitations in computational resources we look at $L = 5$ and fix the initial squeezing parameters to $[1, i, 1, i, 1]$. We first plot the entanglement entropy for a maximum bond dimension of $D = 200$ Fock state propagation (backward propagation).

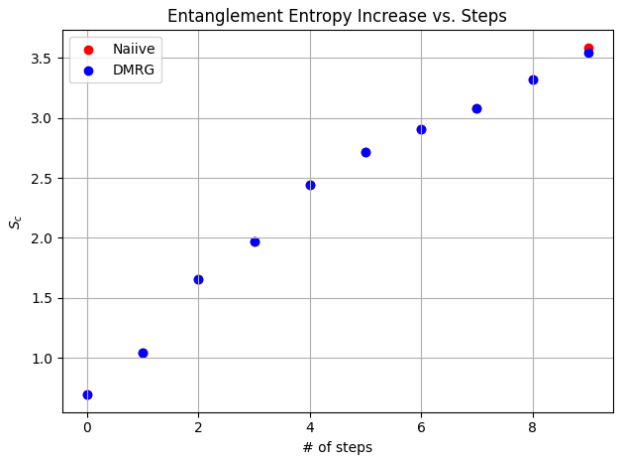

Figure 3: Entanglement entropy at the middle of the MPS for backward propagation methods

Surprisingly, even though the relative error of the DMRG method decreased dramatically (from order of 10^{-2} to order of 10^{-14}), the entanglement entropy in both cases increased in a similar manner. The entanglement entropy increase of the forward propagation method is plotted below.

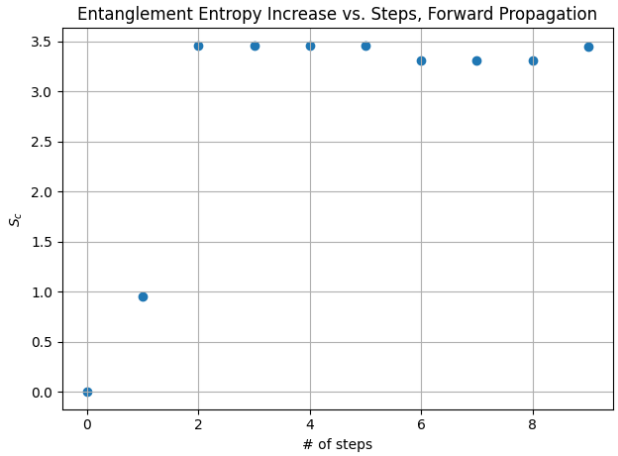

Figure 4: Entanglement entropy at the middle of the MPS for forward propagation methods

The entanglement entropy quickly saturates to a maximum value of $S_c \sim 3.5$. We now plot the bond dimension dependency of the relative error by sweeping various values of $D_{\max}$.

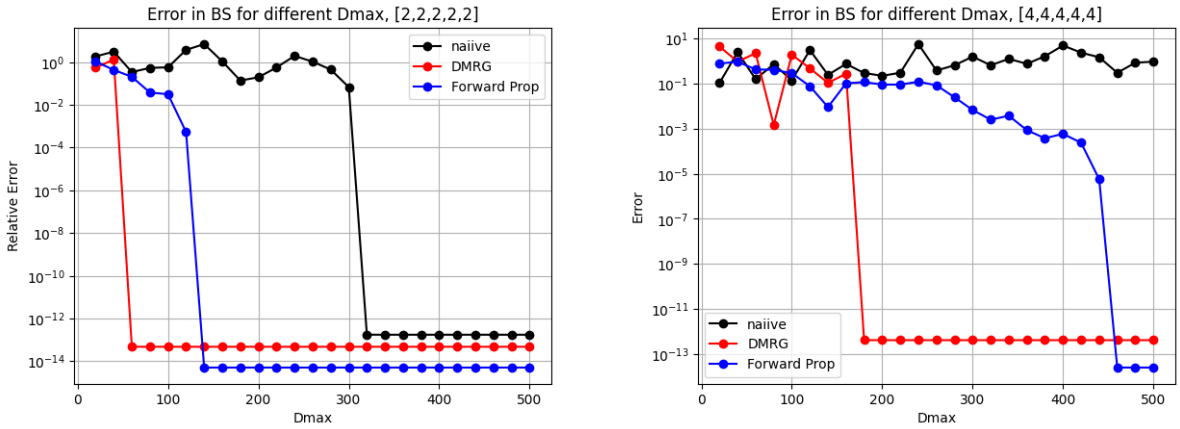

Figure 5: Relative error for different values of $D_{\max}$. We set the measured outcomes as (a) $[2, 2, 2, 2, 2]$ (b) $[4, 4, 4, 4, 4]$ and then calculate the probability.

It is clear that implementing the DRMG method resulted in a decrease in the 'threshold bond dimension' to achieve low error rates. We find that for larger number of photons, the bond dimension must be increased. This is expected, as the number of photons directly is related to the size of the local Hilbert space. Below is a time benchmarking from the same computations. The results may vary for different systems.

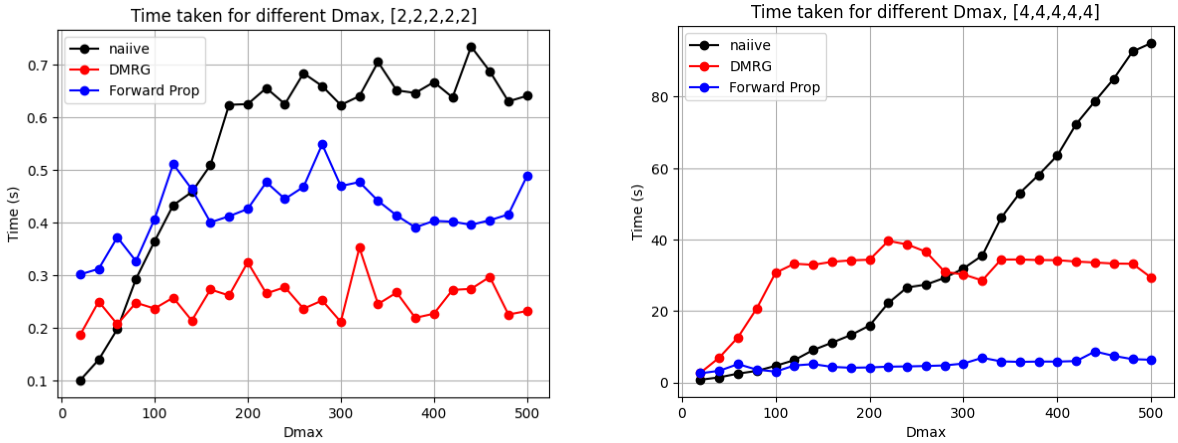

Figure 6: Time taken for different values of $D_{\max}$. We set the measured outcomes as (a) $[2, 2, 2, 2, 2]$ (b) $[4, 4, 4, 4, 4]$ then calculate the probability.

We increased the number of photons and measured the total time taken. We also measure the time taken to directly calculate the probability using the hafnian and plot it alonside the others. For each calculation, the maximum bond dimension was set to $D_{\max} = 200$.

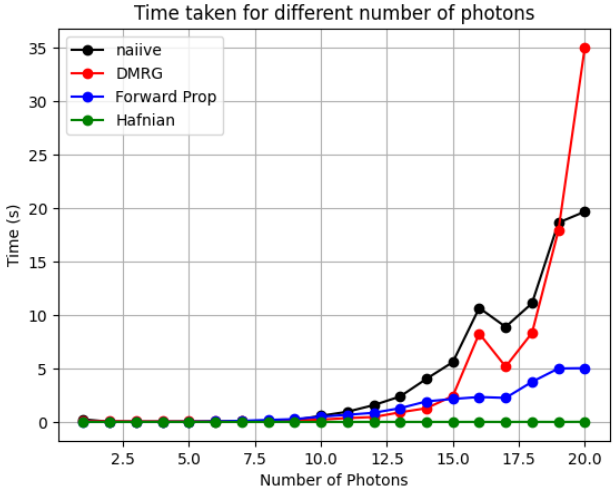

Figure 7: Time taken for various number of photons

It is evident that the direct calculation outperforms all other methods. However, since the time complexity of calculating the hafnian is roughly $O(2^{N/2})$ where N is the number of photons, we suspect the time taken to calculate the hafnian will increase exponentially for large photon numbers. We extend the plot above to photon numbers reaching ~ 40, and compare the hafnian calculation time with the forward propagation time, which was the best performing tensor network-based algorithm. We have plotted the comparison below.

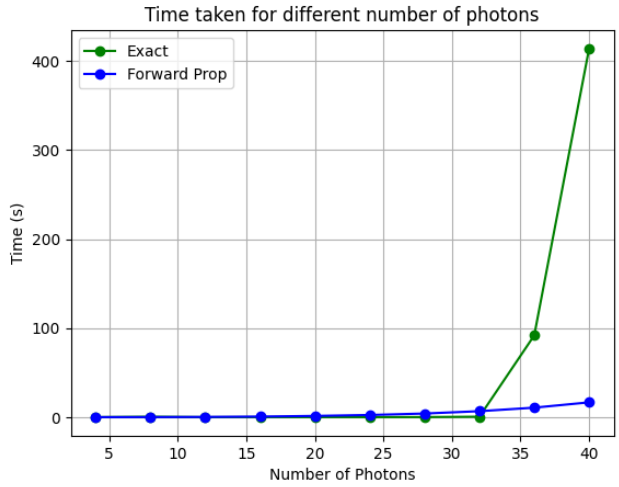

Figure 8: Time taken for various numbers of photons extended up to $N = 40$

We can see a clear exponential relation between calculation time and number of photons for exact calculation, whereas the forward propagation method results in a less severe increase in time complexity. Finally, the 'threshold bond dimension' needed to bring the relative error to an order of 10^{-6} was calculated.

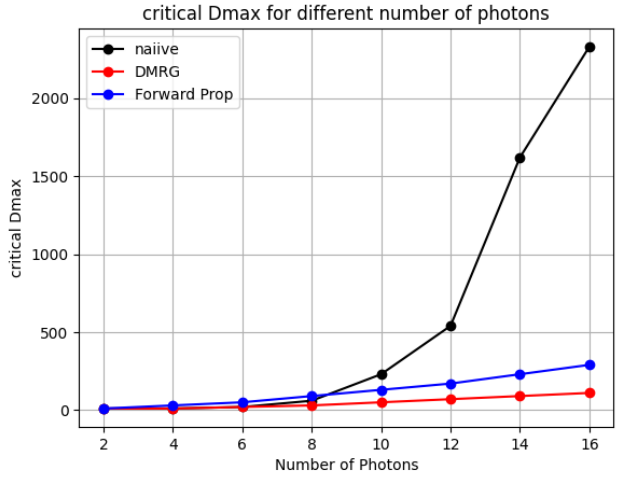

Figure 9: Critical $D_{\max}$ to bring error down to 10^{-6}

4 Discussion

We have constructed two methods of propagating quantum optical states through a linear optical circuit, which is known to be computationally difficult. We have confirmed that our method provides minimal error compared to the explicit calculations. In all cases, the entanglement entropy measured at the middle of the MPS, increased significantly. A surprising result was obtained when implementing the DMRG-styled contraction did not result in a decrease in entanglement entropy, even though the 'threshold bond dimension' needed to

bring the error below 10^{-6} decreased significantly. For forward propagation methods, the entanglement entropy saturates to ~ 3.5 rapidly. We have also plotted the time taken to calculate the results for each method separately. We find that for small values of L and photon numbers, we find that the forward propagation method outperforms the backward propagation methods with DMRG. We also find that directly calculating the hafnian outperforms all tensor network methods, but we suspect that this is due to computational and time restrictions. We support this claim by analyzing computational time as photons number increases to approximately ~ 40. A clear exponential time complexity was found in hafnian calculations whereas the forward propagation scaled much more slowly. Finally, we empirically measured the minimum bond dimension required to achieve low error rates.

Further improvements can be made to decrease the computational load and increase the accuracy. First, we have tried to adapt the localization method introduced in [4] for boson systems to suppress the growth of entanglement entropy. However, the methods proposed in the papers did not yield the same GBS probability values. We suspected this was due to the bosonic Fock space (unlike the fermionic Fock space) not satisfying commutation relations after a basis transformation, we were not able to provide a clear and concise reasoning behind this failure, implying that such a process could be adapted in other ways to avoid this issue. Also, we have tried to implement the DMRG algorithm [5] (first proposed to apply to quantum circuits) to the forward propagation method but failed to create accurate results. Such a method may be more efficient and lead to accurate results, even at lower bond dimensions.

While we have failed to outperform the optimized calculation of the hafnian, our method holds value because we can calculate the explicit evolution through a linear optical circuit. Our first method can be utilized to calculate the Fock probability distribution for an arbitrary input without an increase in computational complexity. This is because the majority of computational complexity required is focused on the evolution of the final Fock state and not the input. Therefore, the first method can be extended to include non-Gaussian arbitrary inputs. Because the efficiency of calculating Gaussian boson sampling results rely on the Gaussian nature of the inputs, this can possibly lead to a computational advantage. In a similar manner, we can utilize our second method to calculate an arbitrary linear optical propagation from a non-Gaussian, arbitrary initial state. This may lead the path to more applications that require the linear optical propagation of non-Gaussian input states.

A Clements Design for LOC

Given an $L \times L$ unitary matrix U, we want to find parameters θ_j and ϕ_j such that U is decomposed into a product of $SU(2)$ matrices where each element is

$$T_j \equiv \begin{pmatrix} e^{i\phi}\cos\theta & -\sin\theta \\ e^{i\phi}\sin\theta & \cos\theta \end{pmatrix}$$

Each element acts on the adjacent modes. Each $SU(2)$ element can be implemented using a Mach-Zehnder interferometer, where phase shifters are tuned according to the parameters

θ_j and ϕ_j. To find the parameters, we nullify each off-diagonal component of the lower half of U by multiplying the $SU(2)$ elements. There are unique value of θ and ϕ that make any target element in U zero. We explicitly find these values for the lower triangular elements of U, which correspond to the interferometer parameters. Once in an upper triangle form, U must be diagonal, as unitarity of a matrix is preserved after multiplying another unitary matrix. We can then find single-mode phase shifter parameters and one more matrix that corresponds to this diagonal matrix. Therefore, we have managed to decompose U into a product of single-mode phase shifters and Mach-Zehnder interferometers, which are the two components of a linear optical circuit. A detailed explanation of this algorithm is explained in Clements *et al.*[7] and implemented in Strawberry Fields[8].

References

[1] Scott Aaronson and Alex Arkhipov. The computational complexity of linear optics. *Theory Comput.*, 9(1):143–252, 2013.

[2] Craig S Hamilton, Regina Kruse, Linda Sansoni, Sonja Barkhofen, Christine Silberhorn, and Igor Jex. Gaussian boson sampling. *Phys. Rev. Lett.*, 119(17):170501, October 2017.

[3] Thomas R Bromley, Juan Miguel Arrazola, Soran Jahangiri, Josh Izaac, Nicolás Quesada, Alain Delgado Gran, Maria Schuld, Jeremy Swinarton, Zeid Zabaneh, and Nathan Killoran. Applications of near-term photonic quantum computers: software and algorithms. *Quantum Science and Technology*, 5(3):034010, may 2020.

[4] Ying-Hai Wu, Lei Wang, and Hong-Hao Tu. Tensor network representations of parton wave functions. *Phys. Rev. Lett.*, 124(24):246401, June 2020.

[5] Thomas Ayral, Thibaud Louvet, Yiqing Zhou, Cyprien Lambert, E Miles Stoudenmire, and Xavier Waintal. Density-matrix renormalization group algorithm for simulating quantum circuits with a finite fidelity. *PRX quantum*, 4(2):1, April 2023.

[6] M Reck, A Zeilinger, H J Bernstein, and P Bertani. Experimental realization of any discrete unitary operator. *Phys. Rev. Lett.*, 73(1):58–61, July 1994.

[7] William R Clements, Peter C Humphreys, Benjamin J Metcalf, W Steven Kolthammer, and Ian A Walsmley. Optimal design for universal multiport interferometers. *Optica*, 3(12):1460, December 2016.

[8] Nathan Killoran, Josh Izaac, Nicolás Quesada, Ville Bergholm, Matthew Amy, and Christian Weedbrook. Strawberry Fields: A Software Platform for Photonic Quantum Computing. *Quantum*, 3:129, March 2019.

[9] Brajesh Gupt, Josh Izaac, and Nicolás Quesada. The walrus: a library for the calculation of hafnians, hermite polynomials and gaussian boson sampling. *Journal of Open Source Software*, 4(44):1705, 2019.